JOURNAL OF GEOPHYSICAL RESEARCH, VOL. 102, NO. D3, PAGES 3819–3830, FEBRUARY 20, 1997

Modeling sea-salt aerosols in the atmosphere 2. Atmospheric concentrations and fluxes

S. L. Gong,[1] L. A. Barrie,[1] J. M. Prospero,[2] D. L. Savoie,[2] G. P. Ayers,[3] J.-P. Blanchet,[4] and L. Spacek[4]

Abstract. Atmospheric sea-salt aerosol concentrations are studied using both long-term observations and model simulations of Na^+ at seven stations around the globe. Good agreement is achieved between observations and model predictions in the northern hemisphere. A stronger seasonal variation occurs in the high-latitude North Atlantic than in regions close to the equator and in high-latitude southern hemisphere. Generally, concentrations are higher for both boreal and austral winters. With the model, the production flux and removal flux at the atmosphere-ocean interface was calculated and used to estimate the global sea-salt budget. The flux also shows seasonal variation similar to that of sea-salt concentration. Depending on the geographic location, the model predicts that dry deposition accounts for 60–70% of the total sea-salt removed from the atmosphere while in-cloud and below-cloud precipitation scavenging accounts for about 1% and 28–39% of the remainder, respectively. The total amount of sea-salt aerosols emitted from the world oceans to the atmosphere is estimated to be in the vicinity of 1.17×10^{16} g yr^{-1}. Approximately 99% of the sea-salt aerosol mass generated by wind falls back to the sea with about 1–2% remaining in the atmosphere to be exported from the original grid square (300 × 300 km). Only a small portion of that exported (~4%) is associated with submicron particles that are likely to undergo long-range transport.

1. Introduction

Since sea-salt aerosols not only scatter solar radiation but also participate in cloud processes, the seasonal variation and total loading may have an impact on both local and global climate. The concentration and flux of sea-salt aerosols in the high-latitude North Atlantic is about twice as high as that in Bermuda [*Erickson et al.*, 1986]. This is largely due to the difference in surface wind speed. However, the large difference in sea-salt loading in the atmosphere is likely to affect climate because of the interactions between sea-salt and clouds and solar radiation. Together with biogenic sulphur aerosols, sea-salt aerosols form the natural background aerosol surface area and concentration of cloud condensation nuclei (CCN) in marine areas upon which atmospheric sulphur aerosols are superimposed. In addition, sea-salt aerosol particles are chemical carriers of species containing Cl, Br, I, and S and therefore play a role in the atmospheric cycles of these important elements. The halogens Br and Cl, once mobilized by heterogeneous reactions from sea-salt inorganic forms to reactive gaseous forms (e.g., Br_2, Cl_2) [e.g., *Mozurkewich*, 1995], can play a role in atmospheric ozone depletion and destruction of light hydrocarbons [*Jobson et al.*, 1994]. Thus, in order to understand the impact of anthropogenic aerosols on climate, it is important to model sea-salt aerosols.

[1]Atmospheric Environment Service, Downsview, Ontario, Canada.
[2]Rosenstiel School of Marine and Atmospheric Sciences, University of Miami, Miami, Florida.
[3]Division of Atmospheric Research, Mordialloc, Victoria, Australia.
[4]Earth Sciences Department, University of Quebec at Montreal, Canada.

Paper number 96JD03401.
0148-0227/97/96JD-03401$09.00

Using the mean monthly surface wind speed at a resolution of 5° × 5° over the world oceans and an empirical relationship between atmospheric sea-salt concentration and wind speed at a reference height of 15 m, *Erickson et al.* [1986] calculated the horizontal distribution of atmospheric sea-salt over the world oceans on a seasonal basis. The sea-salt aerosols in the northern hemispheric marine troposphere displayed a substantial seasonal variation (a factor of 2–3 between the boreal winter and summer), while less variation occurred in the high-latitude southern hemisphere and little variation occurred in the equatorial areas. The global sea-salt budget was also estimated [*Erickson and Duce*, 1988]. Dry deposition was calculated as a function of wind speed by the method of *Slinn and Slinn* [1981] and below-cloud wet deposition by a scavenging ratio formulation.

In a previous paper [*Gong et al.*, this issue], an atmospheric sea-salt aerosol model was developed to estimate sea-salt aerosol mass and number concentrations in terms of meteorological conditions generated by a one-dimensional climate model (FIZ-C) [*Therrien*, 1993]. It was found that sea-salt aerosol concentrations are modulated strongly by the local surface wind speed, and to a lesser extent by long-range transport. Both experiments and model predictions [*Gong et al.*, this issue] have shown that the total sea-salt mass concentration can be expressed as an exponential function of surface wind speed but that the parameters of the function depend on the wind and precipitation climatology of an area. In other words, the assumption of a single relationship between sea-salt mass concentration and wind speed used by others [*Erickson et al.*, 1986; *Erickson and Duce*, 1988] entails considerable uncertainties.

Observational data for total aerosol Na^+ mass concentration in the atmosphere are available at a number of global baseline observatories (Figure 1) including Alert in the Arctic [*Barrie*, 1995], Heimaey, Mace Head, Bermuda, Oahu, Palmer Station, and Cape Grim, enabling an assessment of the global sea-salt

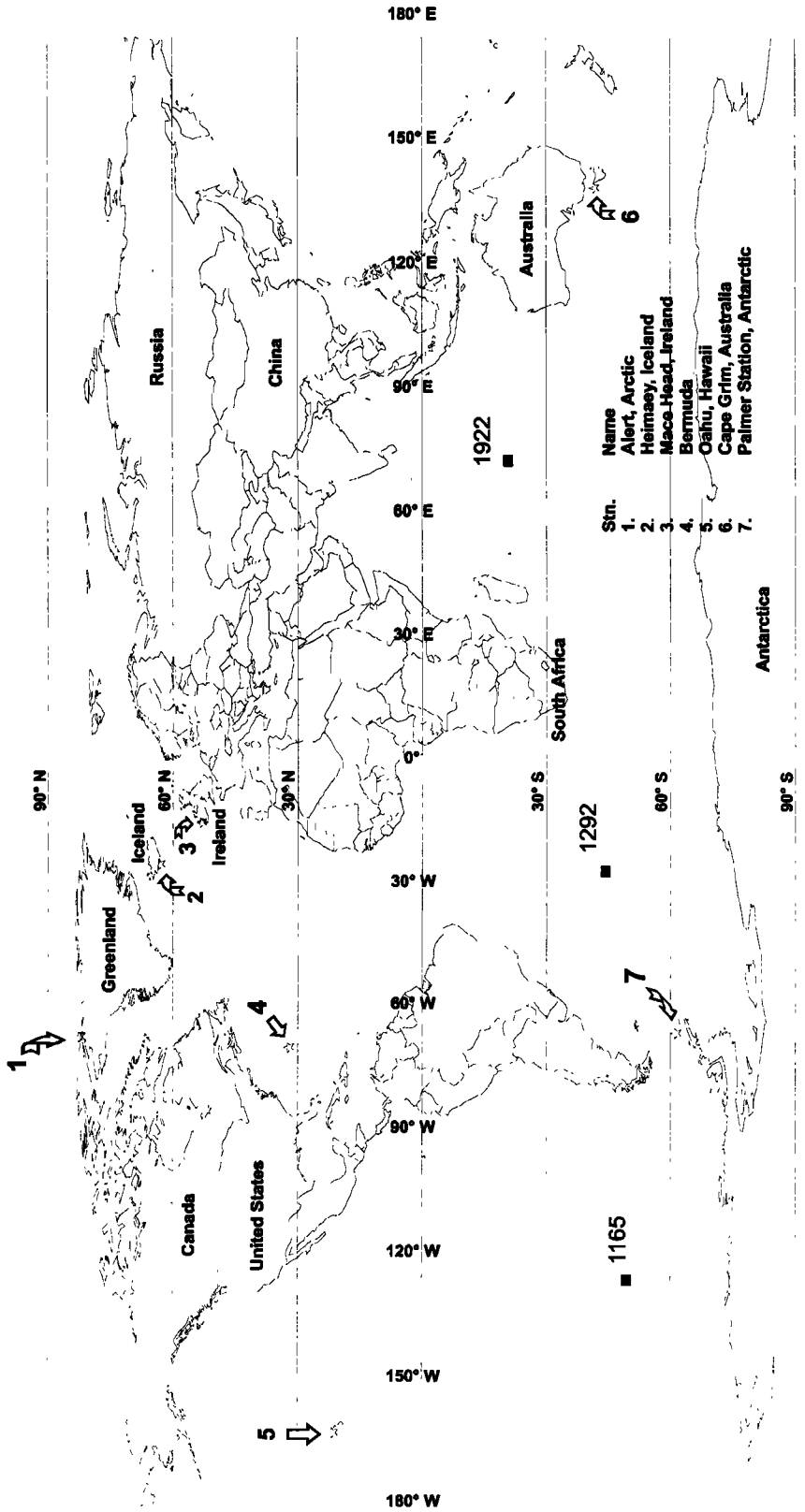

Figure 1. Geographic locations of observation and simulation stations. In addition to the seven baseline observatories, three open oceanic sites in Atlantic, Indian, and Pacific oceans of southern hemisphere are included for the estimate of global sea-salt budget: 1292 (45°S 20°W), 1922 (20°S 80°E), and 1165 (50°S 120°W).

climatology and budget. The aim of this study is to test the ability of our model to predict a realistic surface level sea-salt mass distribution on a global basis and estimate the budget.

The observational data and model predictions are used in a complementary way. Comparison of modelled and observed climatological mean seasonal variation of sea-salt aerosol concentration is needed to test the parameterization schemes used in the model for various atmospheric processes influencing the atmospheric cycle of sea-salt aerosols. Since the size distribution of sea-salt aerosol concentration is resolved by the model, the effect of particle size on major sea-salt aerosol removal processes in the atmosphere such as dry deposition, in-cloud and below-cloud scavenging is investigated. Finally, the model is used to estimate the global sea-salt aerosol.

2. Model Description

A detailed description of the sea-salt aerosol model used in this study is given by *Gong et al.* [this issue]. A brief summary of key features of the model is presented here.

The model includes the following processes: (1) sea-salt generation due to surface wind; (2) vertical transport by turbulence and convection; (3) dry deposition and gravitational settling; and (4) wet removal processes which include both in-cloud and below-cloud scavenging. A one-dimensional climate model (FIZ-C) [*Therrien*, 1993] covering a grid square of 300 × 300 km was coupled with it to provide time-variant meteorological conditions such as surface wind, precipitation, temperature, and relative humidity. Taking the above mentioned processes into consideration, a generalized prognostic mass balance equation for any aerosol type in a discrete size range (i) can be written as

$$\frac{\partial \chi_{ij}}{\partial t} = \left.\frac{\partial \chi_{ij}}{\partial t}\right|_{\text{dynamics}} + \left.\frac{\partial \chi_{ij}}{\partial t}\right|_{\text{surface}} + \left.\frac{\partial \chi_{ij}}{\partial t}\right|_{\text{clear air}} + \left.\frac{\partial \chi_{ij}}{\partial t}\right|_{\text{dry}} + \left.\frac{\partial \chi_{ij}}{\partial t}\right|_{\text{in-cloud}} + \left.\frac{\partial \chi_{ij}}{\partial t}\right|_{\text{below-clouds}} \quad (1)$$

where χ_{ij} is the sea-salt concentration expressed as the mass mixing ratio for ith size range of type j aerosols. In (1), the aerosol concentration change has been divided into tendencies for dynamics, surface, clear air, dry deposition, in-cloud and below-cloud processes. The dynamics includes resolved motion as well as subgrid turbulent diffusion and convection. The surface processes include surface emission of both natural and anthropogenic aerosols and serve as boundary conditions for the model. Particle nucleation, coagulation and chemical transformation are included in clear-air process. It should be emphasized that the resolution of this model is approximately equal to that of the GCMII from which its inputs are derived (300 × 300 km). Thus model predictions represent spatial average concentrations on this scale.

Sea-salt aerosol radius (dry) from 0.03 to 8 μm was divided into eight discrete ranges. For each range, (1) was solved for 10 layers extending from ocean surface to about 33 km in the atmosphere. Except for Alert and Palmer Station which are not situated on the ocean, the model was integrated for each of the points in Figure 1 for 5 years with a time step of 20 min. Monthly averaged sea-salt mass concentration as well as the standard deviation was computed for comparison with the observations. The production flux of sea-salt aerosol mass due to surface wind and removal flux due to dry and wet depositions was extracted from the model results for the first atmospheric layer (0–167 m) and averaged monthly for each size range. Finally, the monthly concentrations, production, and removal fluxes were averaged to yield the monthly mean mass concentrations and fluxes over 5 years. These concentrations and fluxes form the basis for sea-salt trend and budget analysis. In order to compare our predictions with Na^+ concentration observations in the atmosphere, the sea-salt mass concentration is converted into Na^+ mass concentration by assuming that sodium ion content in sea-salt aerosol is 30.77% [*Fergusson*, 1982].

3. Sea-Salt Climatology: Observed and Predicted

3.1. Seasonal Variations of Sea-Salt Aerosols

3.1.1. High-latitude North Atlantic. Two sites in the high-latitude North Atlantic were chosen for this area: Mace Head on the west coast of Ireland (53.19°N, 9.54°W) and Heimaey in Iceland (63.40°N, 20.30°W). The 24-hour mean Na^+ concentrations were measured continuously for 5 years (August 1988 to July 1993) at Mace Head and for 3 years (July 1991 to August 1994) at Heimaey. Observed and predicted monthly averaged Na^+ are compared in Figures 2a and 2b, respectively. At Mace Head, the sampler is sectored toward the west and it should effectively sample winds associated with westerly storms moving through the region. At Heimaey, the sector is from 90° to 270°, encompassing the entire ocean area south of Iceland.

The comparisons are reasonable. Seasonal variations occurred both for the observations and the model predictions for the two points. Sea-salt concentrations are a minimum in the summer time and peak from December to February. However, according to the observations, the seasonal variation is stronger at Heimaey than at Mace Head. The minimum is lower for the model than for the observations. The model performance, defined as the absolute percentage difference between observation and model prediction at the same month, $P_i = |\bar{M}_i - \bar{O}_i|/\bar{O}_i \times 100\%$, ranges from 10% to 160%, depending on month and location. The annual average performance (AAP) is quantified as follows:

$$\text{AAP} = \frac{\sum_{i=1}^{12} P_i}{12} = \frac{\sum_{i=1}^{12} \dfrac{|\bar{M}_i - \bar{O}_i|}{\bar{O}_i}}{12} \times 100\%, \quad (2)$$

where $\bar{M}_i$ is the average concentration for month i from a prediction over the modeling period and $\bar{O}_i$ from an observation over the measuring period. It is 54% and 26% for Mace Head and Heimaey, respectively.

The observed point for February at Heimaey, Iceland, needs some scrutiny since it is much higher than the neighboring months. In the original data, Na^+ concentration was observed for three consecutive Februarys from 1992 to 1994. For February 1992, the monthly averaged Na^+ concentration was 28.0 μg m^{-3} with a standard deviation of 59.8. A concentration as high as 296.3 μg m^{-3} was recorded on February 13, 1992, possibly because of a winter storm. As a result of this high episode, the averaged Na^+ concentration in February was exceptionally high. If this observation is excluded, the curve for the observation in Figure 2b would be much closer to the model predictions.

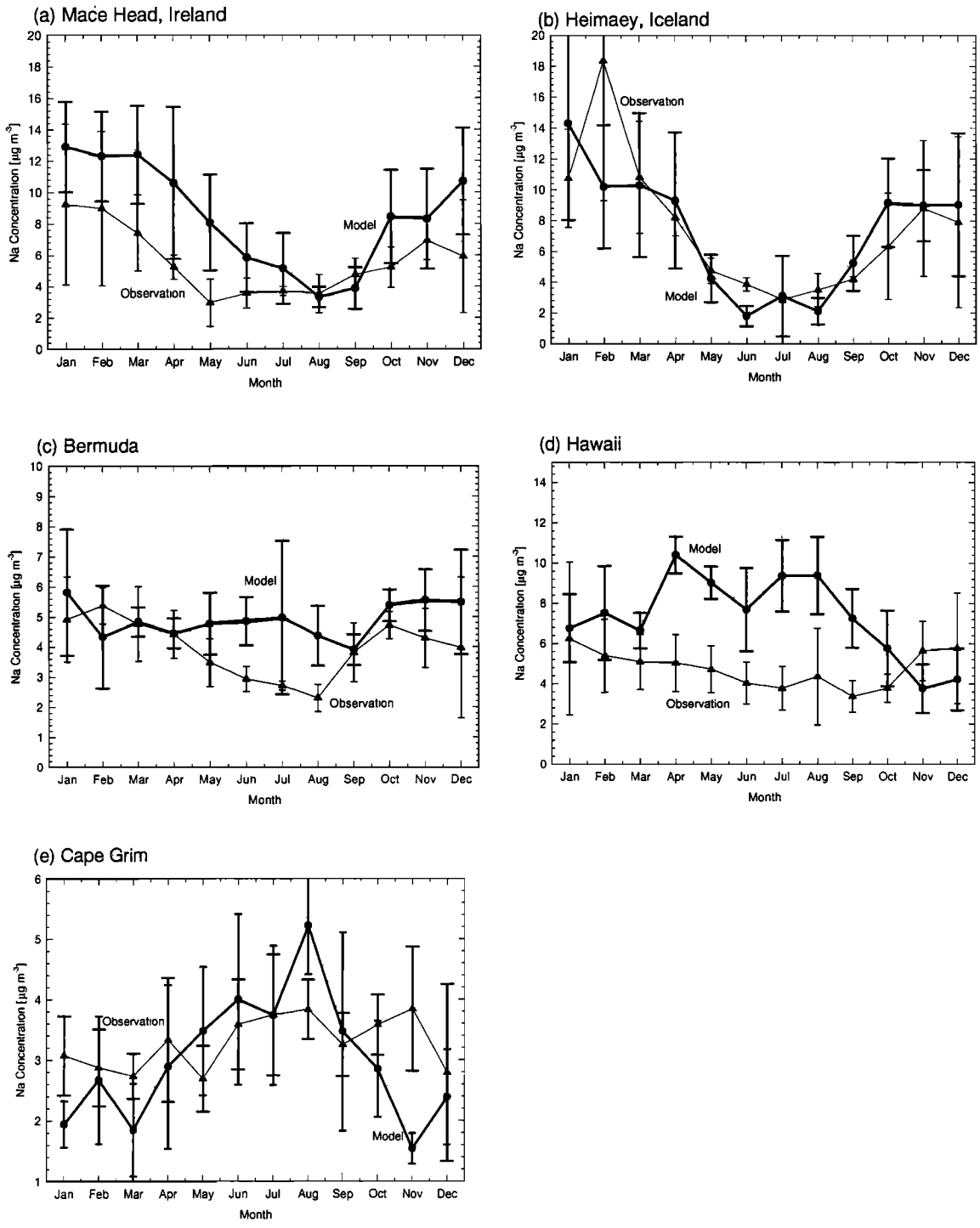

Figure 2. Comparison of monthly mean sea-salt [Na^+] concentrations between observation and simulation. The error bar indicates one standard deviation. (a) Mace Head, Ireland, (b) Heimaey, Iceland, (c) Bermuda, (d) Oahu, Hawaii, and (e) Cape Grim, Australia.

It is worthwhile to point out that due to the coarse resolution used in the FIZ-C (300 × 300 km), some sporadic and extreme events, such as an isolated storm or unusually calm conditions, may not be resolved in the model. On the other hand, such sporadic events, should they occur, will invariably contribute to the actual observations. In a short term, these events may have an effect on the comparison between observations and model predictions. Since sea-salt climatology is the major concern in the paper, these sporadic events should be averaged out over time.

The agreement of seasonal variation between model and observation is not as good at Mace Head as at Heimaey. Two sources of uncertainties exist: model wind speed and representativeness of measurement stations. The first one is that the seasonal variation of wind speed is too large for the grid square including Mace Head. Because of the resolution (~300 × 300

km), the model-derived wind may represent the average wind speed in that area but not for Mace Head which is located on the coast. The associated, second uncertainty revolves around the fact that the wind speed measured at a coastal station such as Mace Head may have a weaker variation than the open ocean winds in that region. This influence can be seen from the predictions of other sites such as Bermuda and Oahu as well.

3.1.2. Bermuda and Oahu. Bermuda (32.27°N, 64.87°W) and Oahu (21.33°N, 157.70°W) are two islands located in the Atlantic and Pacific, respectively. Figures 2c and 2d show the seasonal variations of Na^+ concentrations for the two points. The seasonal variability and the concentration is less than that for high-latitude points such as Mace Head and Heimaey. At both locations, observations show a small decrease of the sea-salt concentration in the summer time, while predictions show no significant decrease for Bermuda and a maximum at Oahu. As opposed to the observations, a peak in summer for Oahu was predicted by the model (Figure 2d). In view of the climatology of wind speed and precipitation at Oahu, the model result is likely justified. In Figure 3, the monthly observed mean wind speed and precipitation data [*Van Loon*, 1984] are plotted for Oahu (21.20°N, 157.55°W) at a 5-m elevation. The higher wind speed and lower precipitation in the summer time should produce a maximum sea-salt concentration as predicted by the model rather than a minimum concentration as observed. It should be pointed out that the sampler at Oahu is sectored toward the north. This may bias against the summer winds which are associated with southeastly trades at Oahu.

Nevertheless, in terms of annual average values the agreement between model predictions and observations for the two sites is reasonable. AAP is 33% and 71% for Bermuda and Oahu, respectively.

3.1.3. Cape Grim in the southern hemisphere. The Na^+ trend at Cape Grim (40°41'N, 144°41'E) on the northwest tip of Tasmania from our 5-year simulation and in situ measurements is shown in Figure 2e. The experimental data (Baseline Atmospheric Program (Australia), Bureau of Meteorology and CSIRO Division of Atmospheric Research, Annual Reports, 1976–1991) were taken from December 1988 to May 1993 by a sampler with PM_{10} hivol head to remove particles with radius larger than 5 μm. A 7-day sampling interval was used during this period. In Figure 2e, the observations and predictions of sea-salt aerosol concentration are shown for $r \leq 5$ μm.

A general agreement was achieved between the observations and model predictions in terms of the annually averaged Na^+ mass concentration. The AAP for Cape Grim is 22%. Little seasonal variation was observed in the experiment at Cape Grim. The observed annual average Na^+ concentration is 3.3 $\mu g\ m^{-3}$ while the model predicts an annual average of 3.0 $\mu g\ m^{-3}$ for sea-salt particles of less than 5 μm in radius. However, a seasonal variation of sea-salt aerosols was predicted by the model. The maximum concentration was obtained during the months of July to October. This maximum is mainly caused by the high wind speed from the climate model. As was pointed out by *Erickson et al.* [1986] the seasonal variation of Na^+ concentration in the midlatitude southern hemisphere is much less than that in the northern hemisphere.

3.1.4. Alert in the Arctic and Palmer Station in the Antarctic. Unlike the other stations discussed above, these two sites are remote from ocean water. Consequently, the concentrations observed are not directly comparable to the one-dimensional model predictions since the model does not simulate removal during transport to the sites over ice-covered terrain. Figure 4a shows the monthly averaged Na^+ air concentration observed at Alert over 13 years [*Barrie*, 1995]. Minimum concentrations are observed in summer time (June–August). The sea-salt aerosol peaks over a broader winter period beginning in early October and ending in April. Being far away from the open ocean, the Na^+ in Alert is mainly contributed from long range transport. *Barrie and Barrie* [1990] attributed the winter peak to a combination of longer aerosol residence times and stronger sea spray sources in the northern oceans at that time of year than in the summer. This is clearly shown in Figures 2a and 2b where the sea-salt production is at a maximum in the high-latitude North Atlantic ocean during boreal winter and a minimum in the summer.

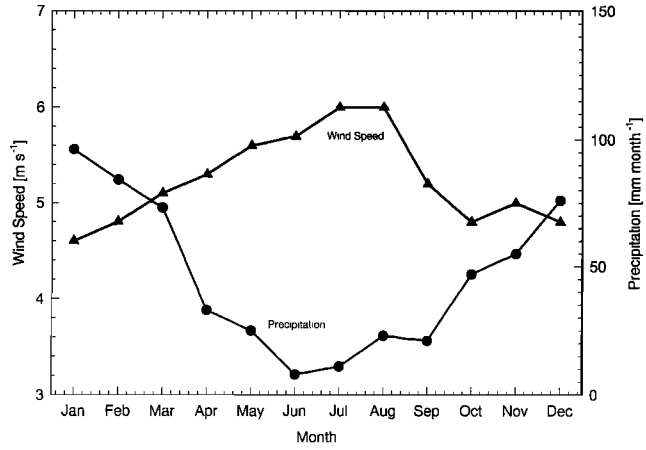

Figure 3. Observed monthly mean wind speed and precipitation data at Oahu, Hawaii.

The Na^+ concentrations at Alert are ~60 times lower on average than at sites close to open ocean (compare Figures 2a, 2b, and 2c). As pointed out by *Gong et al.* [this issue], most of the large particles (e.g., r = 4–8 μm) generated over open ocean have a short atmospheric residence time (~1/2 hour) and are unlikely to survive long-range transport to Alert over Arctic ocean ice [*Barrie et al.*, 1994]. Aerosols at Alert are associated with smaller sea-salt particles (mass median diameter ~1 μm) which represent only a small portion of sea-salt aerosol mass generated at the source. There is strong correlation (Figure 4a) between Na^+ air concentration at Alert and the production rate of sea-salt at Heimaey, Iceland. This is consistent with transport of sodium aerosols from high-latitude North Atlantic ocean to Alert.

Although, observed Na^+ is approximately 5 times higher at Palmer Station in the Antarctic than at Alert in the Arctic (Figure 4), it is still lower than predicted from the open ocean point about 600 km north of the Palmer Station (Figure 4b). This is due to removal as discussed above but over a shorter distance than to Alert.

3.2. Sea-Salt Flux and Budget at the Sea-Atmosphere Interface

Compared with observations, the model predicted not only a reasonable seasonal variation of sea-salt mass concentration for some locations but also a rather consistent yearly averaged concentration throughout the 5-year simulation as indicated by the values of AAP for various stations. This agreement demonstrates that the parameterization schemes used for sea-salt generation and removal processes and the climatology gener-

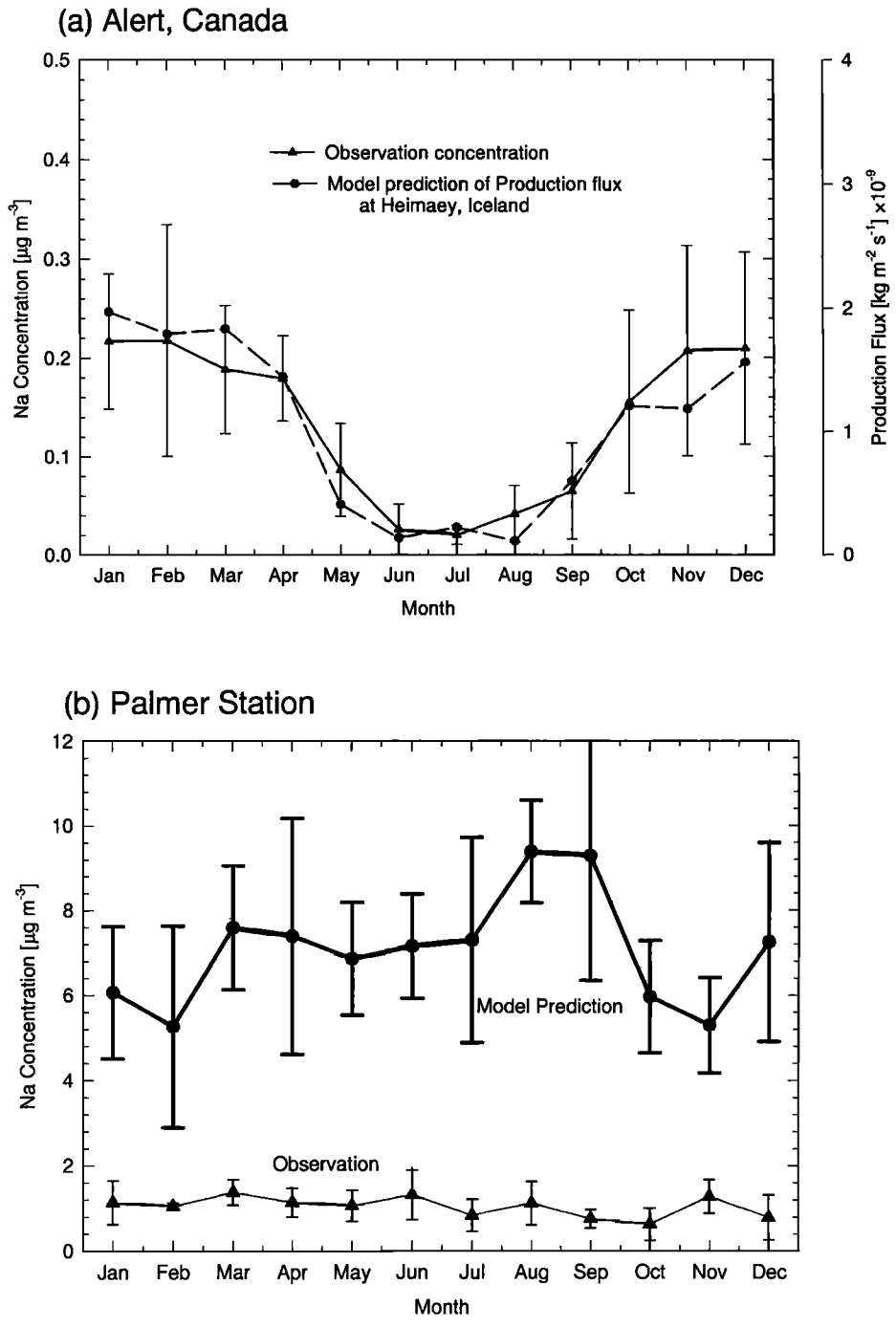

Figure 4. (a) Monthly mean sea-salt [Na^+] concentrations at Alert, the Arctic from observations. The production flux of sea-salt aerosols at Heimaey, Iceland, is also shown. The error bar indicates one standard deviation. Note that a different scale are used for the flux. (b) Comparison of monthly mean sea-salt [Na^+] concentrations between observations at Palmer Station, Antarctic, and a model prediction 600 km north of Palmer Station.

ated by the FIZ-C climate model are reasonable. In this section, a flux and budget analysis of sea-salt aerosols is presented. The production flux for different size ranges as a function of surface wind speed was calculated dynamically in our model using the empirical parameterization of *Monahan et al.* [1986]. Dry deposition, gravitational settling, and wet removal contributed to the removal flux of sea-salt aerosols. The fluxes in units of kg m^{-2} s^{-1} were calculated at each time step and averaged monthly.

3.2.1. Seasonal variation of sea-salt flux. The model results show a strong seasonal variation of sea-salt concentration at Mace Head, Heimaey, and a small weaker one at Bermuda, Oahu, and Cape Grim. These variations are associated with the seasonal variations in surface production and atmospheric removal of sea-salt aerosols. In Figure 5, the seasonal trend for the monthly surface production flux and the ratio of removal/production flux are presented for Mace Head, Heimaey, Bermuda, Oahu, and Cape Grim, respectively. For Mace Head

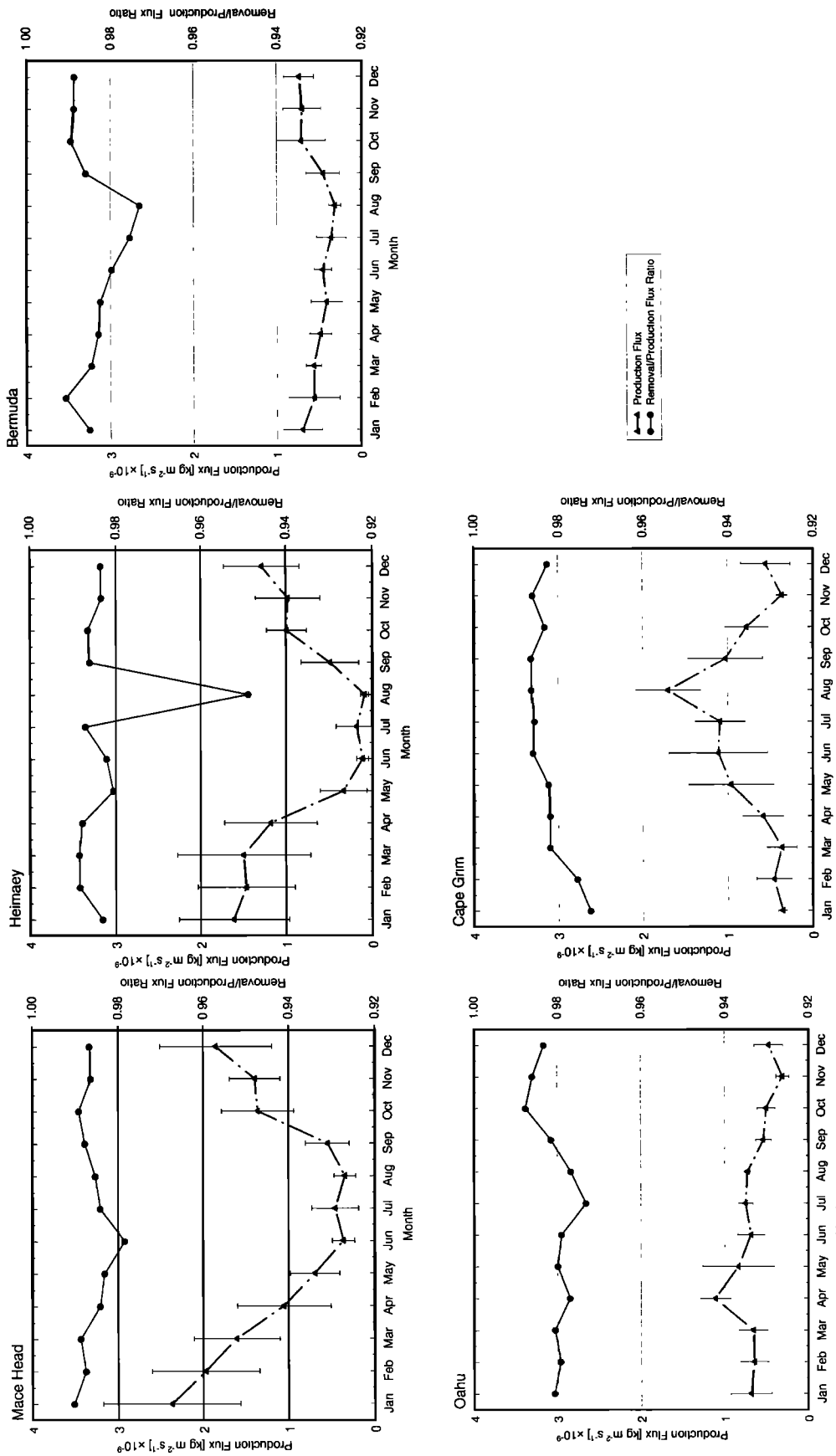

Figure 5. Seasonal variation of sea-salt production flux and the ratio for removal/production flux at Mace Head, Heimaey, Bermuda, Oahu, and Cape Grim. The error bar indicates one standard deviation from simulation results.

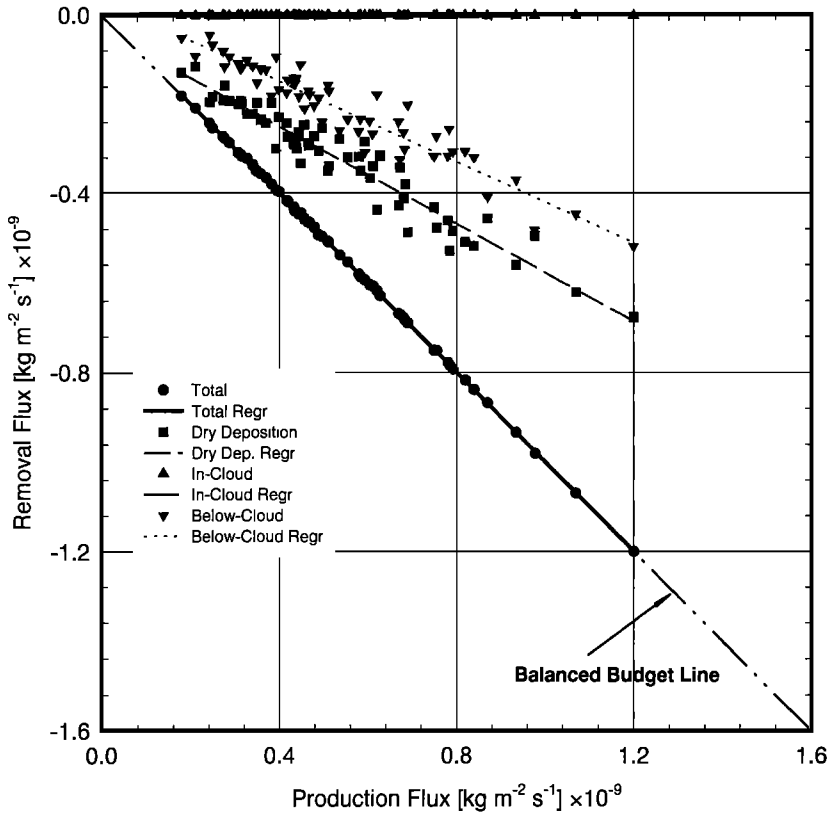

Figure 6. Correlation between removal and production flux at Bermuda for different removal processes. Each marker in the plot represents a monthly averaged value.

and Heimaey, the minimum flux during June to September corresponds to the minimum mass concentration of sea-salt aerosols in the same period obtained from both observation and model prediction. Production flux at Bermuda is similar to that at Mace Head and Heimaey with less seasonal variation and smaller magnitude. This implies that the cycling of sea salt in the atmosphere in the high-latitude North Atlantic is much more intensive than at Bermuda. The seasonal variation of production flux in Oahu differs slightly to that in Bermuda and the North Atlantic. A higher flux between April and August was obtained. Although the trend does not agree well with the observation, it is supported by the climate data for that region (Figure 3). An explanation has been given in subsection 3.1.2. for the discrepancy.

Cape Grim is the only simulation point located in the southern hemisphere. Taking into account austral winter being 6 months out of phase in the southern hemisphere, Cape Grim has a similar variation to the northern hemispheric sites. Higher production flux was associated with winter months of May to September.

The analysis in this study for the seasonal variation of atmospheric sea-salt concentration and flux generally agrees with that by *Erickson et al.* [1986]. They found that seasonal variation in the northern hemisphere is higher than that in the high-latitude southern hemisphere. The smallest seasonal variation is found around the equatorial region. The variability predicted by our model at Cape Grim in the southern hemisphere was not evident in the observations.

The ratio of removal to production flux at the ocean/atmosphere interface is also shown in Figure 5 for each site. This ratio indicates the degree of atmospheric removal of sea-salt aerosols in the grid square. As can be seen from Figure 5, the mean ratio is between 0.98 and 0.99 for all sites and does not vary substantially with season except for August at Heimaey where the ratio is 0.95.

3.2.2. Sea-salt budget. The budget of sea-salt aerosols is investigated in two scales: local grid scales and global average.

Local budget: For each point, the removal flux was separated into dry, in-cloud and below-cloud flux. In Figure 6, the surface production flux at Bermuda is compared to the removal flux of total mass (r = 0.03–8 μm). The removal flux of total mass correlates very well with the surface production flux (slope = −0.99). A very small fraction of the production flux is not balanced, probably due to vertical movement of smaller particles by turbulent diffusion that contribute only a little to total mass. Dry deposition contributes more than 60% to removal of total sea-salt mass. Of wet scavenging, in-cloud and below-cloud scavenging processes accounts for 1% and 30%, respectively.

In the literature, there exists a very large range in estimates of relative contributions of dry and wet removal processes to total sea-salt removal. *Erickson and Duce* [1988] estimated an annual rate of 1.5 × 10^{16} g for global dry deposition and 1.8–6.0 × 10^{15} g for global wet deposition. This corresponds to 70% dry and 30% wet removal. *Blanchard*'s [1963] computation yielded a global dry deposition of atmospheric sea salt of 3 × 10^{15} g yr^{-1} and wet deposition of 6 × 10^{15} g yr^{-1}. This corresponds 33% dry and 67% wet removal. There are several reasons for this difference. First, the dry deposition rate either by measurement or by model calculation differs a lot between

Table 1. Annual Sea-Salt Removal Flux Fraction at Various Stations

Station	Dry Deposition	In-cloud	Below-cloud	Slope*
Bermuda	60%	1.0%	39%	−0.99
Cape Grim	68%	1.0%	31%	−0.99
Heimaey	67%	1.0%	32%	−0.98
Mace Head	68%	1.0%	31%	−0.98
Oahu	71%	1.0%	28%	−0.97

*The slope is for the regression line of downflux upflux. A value of −1.000 means complete removal.

these two studies. Spatial and temporal variation of dry deposition rate is not understood well. The uncertainty in dry deposition rate will inevitably affect the fractional loss. In addition, the concentration used by *Erickson et al.* [1986] to calculate the flux was based on the global wind distribution and a single equation relating wind speed and sea-salt mass concentration. The equation chosen may not necessarily apply globally as both measurements and model predictions have indicated that there exists a different relationship between sea-salt mass concentration and wind speed for different locations [*Gong et al.*, this issue]. Furthermore, a single value of 500 for the scavenging ratio in the wet deposition calculation [*Erickson et al.*, 1986] would result in a large uncertainty.

Our prediction agrees best with the prediction of *Erickson and Duce* [1988]. According to our simulation, similar relative removal by dry and wet depositions was obtained for all stations. Table 1 summarizes the production flux, separated removal flux, and the correlation between production and removal flux for different stations. Dry deposition contributed more to the major removal processes of total sea-salt aerosols than wet removal. Since no clouds are allowed in the lowest model layer (e.g., 0–166 m) in FIZ-C physics to prevent development of excessive low cloudiness [*McFarlane et al.*, 1992], the in-cloud removal fraction is quite small, that is, 1–2%. It is attributed to the in-cloud removal of sea-salt from the second lowest layer and above.

Note that in all cases removal did not match production, that is, ~1–2% of mass generated at the surface remained in a column above the grid square (300 × 300 km) of the FIZ-C. This unbalanced mass enables sea-salt aerosols to be exported beyond the grid square and to engage in long-range transport. This is consistent with observations of sea-salt aerosol at sites remote from open ocean such as Alert and Palmer Station. To investigate the size dependence of this net export, we considered size-segregated production and removal fluxes in the model. Figure 7 shows the correlation between production and removal flux for eight size ranges at Bermuda. For all particle size ranges, the production flux is nearly balanced by the removal flux. In view of the wide size spectrum considered in the model (r = 0.03–8 μm), there exists more than one dominant removal mechanism for large and small aerosol particles. This is clearly shown in Figure 8 where the size-segregated removal fractions of three processes for eight size bins are plotted at Bermuda for the month of January. The fractions in the graph reflect the relative importance of three removal processes of sea-salt aerosols at different sizes. For large particles (r = 0.5–8 μm), dry deposition accounts for more than 50% of the total removal process and is the dominant removal mechanism. Because of their large dry deposition velocity, these particles will fall back to the sea surface in a very short time. *Gong et al.* [this issue] calculate an atmospheric residence time of several hours for these particles. The remaining removal fraction

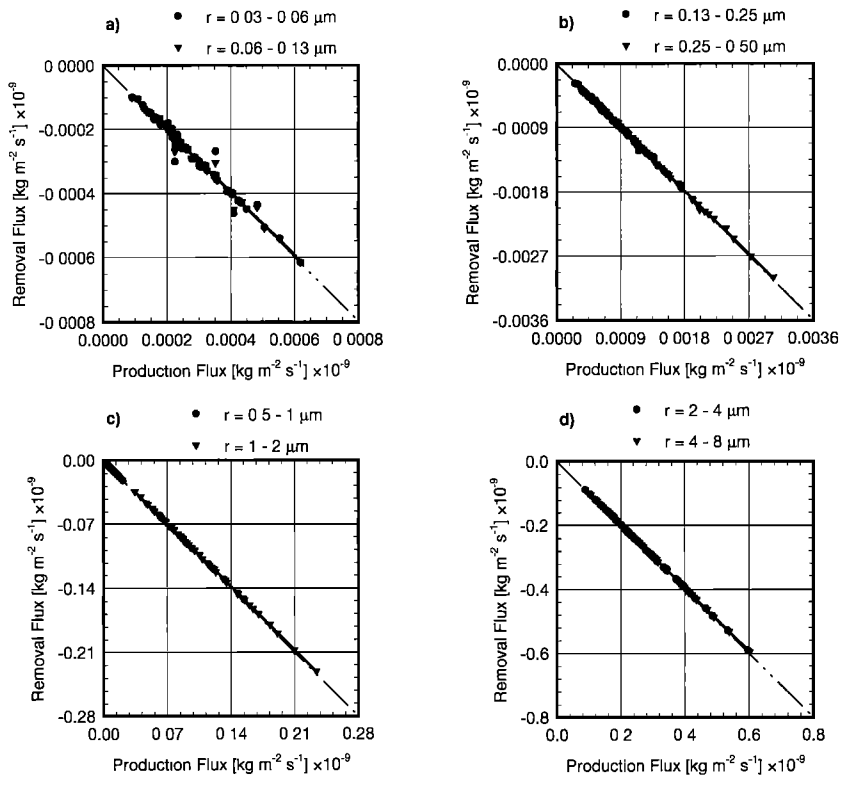

Figure 7. Size-segregated correlation between removal flux and production flux at Bermuda. Each marker in the plot represents a monthly averaged value.

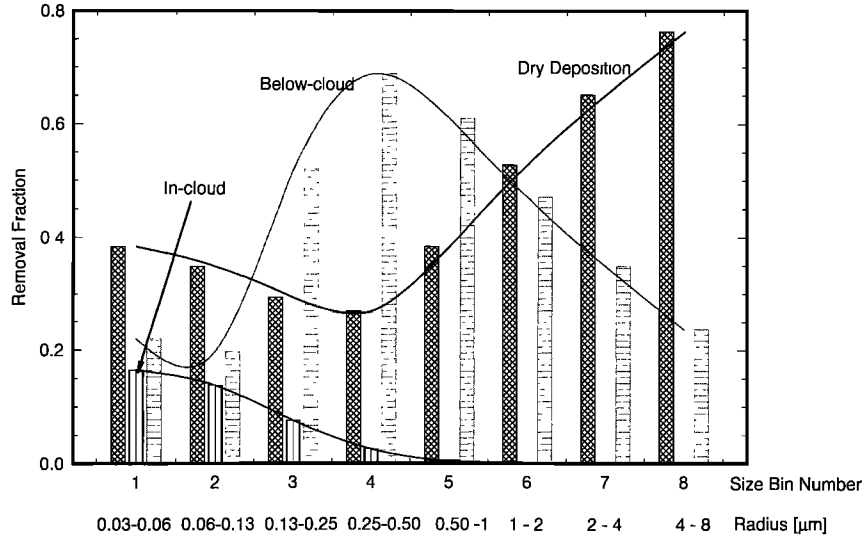

Figure 8. Size-segregated fractional loss for three separated removal processes.

(~40%) of particles in these size ranges is attributed to the below-cloud removal processes. For smaller particles in bins 1–4 (r = 0.03–0.5 μm), the dry deposition velocity is much lower and the wet removal processes become comparable to the dry deposition. For sea-salt aerosols in these size bins, the combined below- and in-cloud scavenging accounts for more than 60% of total sea-salt mass removed from the atmosphere.

In terms of mass fluxes which cycle through the atmosphere/ocean interface, large particles (r = 0.5–8 μm] dominate (Figures 7c and 7d) both generation and removal processes. The flux for these particles is much larger than that in Figures 7a and 7b. To gain further insight into the cycling process, the unremoved number flux and mass fraction of sea-salt aerosols in each size bin was calculated at Bermuda (Figure 9). About 96% of the total unremoved mass is attributed to particles larger than 1 μm in diameter (r = 0.5–8 μm) with remaining fraction attributable to the submicron particles. Because of their short residence time (<1 day) in the atmosphere, most of the particles in bins 5–8 (r = 0.5–8 μm) will not be transported far from their source grid. On the other hand, submicron sea-salt aerosols have a long atmospheric residence time and are likely to be transported by turbulent motion of the air into the higher atmosphere and later engaged in long-range transport by advection. This is consistent with the observation of Na^+ aerosols at Alert [*Barrie et al.*, 1994] which shows aerosol concentration about 60 times lower than in open oceanic regions and a particle mass median diameter of Na^+ below 1 μm [~0.49 μm]. The analysis seems to suggest that although the large particles contribute most of total unremoved sea-salt mass, only a small fraction [4%] of it [due to sub-micron particles] will participate in long range transport and be exported from oceans to surrounding ice or land surfaces. In contrast to the mass fraction, however, the sub-micron particles dominate the number flux of unremoved sea-salt aerosols (Figure 9).

Global budget: The production and removal fluxes of sea-salt aerosol at the sea/atmosphere interface enable us to estimate the global sea-salt budget. In addition to the five simu-

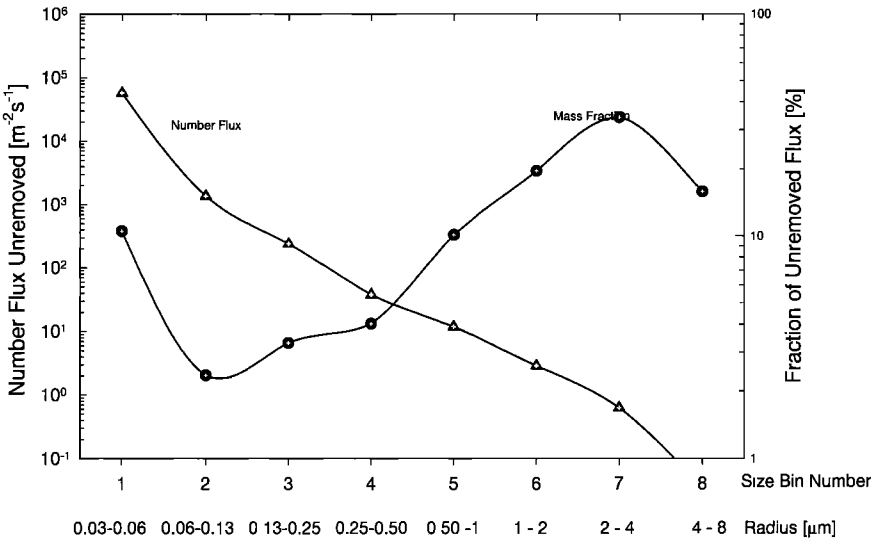

Figure 9. Size-segregated unremoved mass fraction and number flux at Bermuda.

Table 2. Global Sea-Salt Annual Flux Estimate

	Northern Hemisphere				Southern Hemisphere				Best Estimate*
	Mace Head	Heimaey	Bermuda	Oahu	Cape Grim	1165	1292	1922	
Dry	8.9	6.4	3.6	5.2	6.0	13.6	11.3	6.1	7.9
In-cloud	0.10	0.10	0.06	0.06	0.07	0.14	0.11	0.07	0.08
Below-cloud	4.0	3.0	2.1	2.1	2.7	5.9	4.1	2.6	3.4
Total Out	13.1	9.5	7.3	7.3	8.8	19.6	15.6	8.9	11.5
Total In	13.3	9.6	7.5	7.5	8.9	19.9	15.8	9.0	11.7
Net Input	0.17	0.14	0.10	0.15	0.14	0.30	0.20	0.16	0.17

Estimates are in g $yr^{-1} \times 10^{15}$.

*The best estimate was obtained by $F_B = 0.428\bar{F}_{North} + 0.572\bar{F}_{South}$, where $\bar{F}_{North}$ and $\bar{F}_{South}$ are the averaged flux for northern and southern hemisphere, respectively. The fractions of world ocean at northern and southern hemisphere are 0.428 and 0.572.

lation points (station 2, 3, 4, 5, and 6 of Figure 1) used above, three more points in the southern hemisphere (1165, 1292, and 1922 in Figure 1) were added to estimate the global distribution. Using an apparent area of the world ocean of 3.61×10^{18} cm^2 [*Baumgartner and Reichel*, 1975], the annual production and removal rates of global atmospheric sea-salt aerosols were calculated by integrating the production flux and removal flux of each station over 12 months. The estimated values are listed in Table 2.

The model-predicted annual sea-salt removal rate from the atmosphere was estimated to be 1.15×10^{16} g of which dry deposition, in- and below-cloud account for 7.9×10^{15} g, 8.0×10^{13} g, and 3.4×10^{15} g, respectively. These values were calculated from the weighted average fluxes over northern and southern hemispheres by considering the fraction of the world ocean in both hemispheres. The relative contributions of dry, in- and below-cloud to total annual removal are 69%, 0.7%, and 30%, respectively. The annual production rate of sea-salt from the ocean to the atmosphere is 1.17×10^{16} g. The difference between production and removal rates yield a global atmospheric net input of sea-salt of 1.7×10^{14} g yr^{-1} from the world oceans. This is the amount of sea-salt aerosols unremoved in the atmosphere over the oceans and likely exported to the continents. Because of one-dimensional nature of the climate model, the net input may reflect some uncertainties since the horizontal advection is not considered in the model.

Despite different techniques used to arrive at a global sea-salt flux, the value estimated from our model is comparable with estimates from previous studies. The removal rate estimated by *Erickson and Duce* [1988] is 1.8×10^{16} g yr^{-1}. Assuming a global dry deposition flux of atmospheric sea-salt aerosols of 5.5×10^{-6} $\mu g\ cm^{-2}\ s^{-1}$ and that the trade wind regions were representative of the global wind field, *Eriksson* [1959] estimated the global sea-salt production to exceed 1.0×10^{15} g yr^{-1}. By a similar but improved approach, *Blanchard* [1963] gave the annual removal rate of 9×10^{15} g yr^{-1}. In an attempt to calculate the budget of sea salt and sulfur in the atmosphere, *Petrenchuk* [1980] estimated the intensity of sea-salt aerosol sources of 1.3×10^{15} g yr^{-1}. Using the whitecap atlas, *Spillane et al.* [1986] estimated the annual sea-salt mass flux to be 3.50×10^{15} g.

Another important parameter relevant to the global sea-salt budget is the net export of sea-salt to the land surfaces. Our estimate from the model is 1.7×10^{14} g yr^{-1}. River runoff of chloride was used to approximate the quantity of chloride deposited on land from the ocean [*Eriksson*, 1960; *Petrenchuk*, 1980]. By this method, *Eriksson* [1960] estimated a value of 1.01×10^{14} g yr^{-1} for an annual net export of sea-salt to the land surface, while *Petrenchuk* [1980] increased the value to 3.70×10^{14} g yr^{-1}. Two factors affect the accuracy of this estimate. First, river run-off of chloride is contributed not only by sea-salt deposition on the land surface but also by industrial activities along rivers, dry soil salts, igneous rocks and more. The extent of contributions other than sea-salt is very difficult to estimate. Second, a sea-salt budget estimate based on chloride river run-off suffers the weakness of local effects. The sampling locations and time all have an influence on the global average value. A better method for the net export is to calculate the dry and wet deposition of sea-salt aerosols on global land surfaces. Since the net export involves both the production and transport of sea-salt aerosols, a three-dimensional global climate model is ultimately required to couple with this aerosol model for a more accurate global sea-salt budget estimate.

The general agreement between modeling and observation climatology of sea-salt aerosols as presented above with a one-dimensional climate model indicates that a much better value for global sea-salt budget can be achieved if the model is coupled with a three-dimensional global GCM. It is anticipated that global sea-salt production, deposition, and transport will be calculated dynamically in the model and global sea-salt budget is thus obtained dynamically. The initial effort at such a global three-dimensional run is currently being undertaken at Atmospheric Environment Service of Canada. The Northern Aerosol Climate Model (NARCM) covering most of anthropogenic aerosol source regions in the northern hemisphere (>35°N) and having a resolution of 1° × 1° is being developed with this aerosol model and used to study the production, removal, and transport of sea salt, sulphur, and soil dust aerosols.

4. Conclusions

Both observations and model predictions demonstrate that atmospheric sea-salt aerosol concentrations have seasonal variations whose magnitude depends on the geographic location. Sea-salt concentrations in the high-latitude North Atlantic (Mace Head and Heimaey) show a substantial seasonal change. The seasonal dependence is decreased in lower-latitude regions (Bermuda and Oahu). Higher sea-salt concentrations are generally found in boreal winters except for Oahu where higher concentration is predicted in summer time by the model. The sea-salt concentration at Alert in the high Arctic resembles the seasonal variation in the high-latitude North Atlantic but is ~60 times lower. Observations at Palmer Station in the Antarctic and Cape Grim revealed little seasonal variations.

Depending on the geographic location, model estimates indicate that dry deposition accounts for 60–70% of the total sea-salt removed from the atmosphere while in-cloud and below-cloud precipitation scavenging is responsible for ~1% and ~30% of the total removal. Size-segregated removal flux analysis shows that only 1–2% of the total sea-salt mass emitted from the ocean surface in all size ranges (r = 0.03–8 μm) remains in the column above the grid square as a net input to the atmosphere. Of the net input sea-salt aerosols, particles of radius r = 0.5–8 μm contribute most of the mass (96%) with the remaining 4% coming from submicron particles in the radius range, r = 0.03–0.5 μm.

The total amount of sea-salt aerosols emitted from the world oceans to the atmosphere is estimated to be 1.17×10^{16} g yr^{-1}, while the annual removal of sea-salt aerosols is calculated to be 1.15×10^{16} g. This estimate is quite consistent with previous estimates found in the literature.

In view of the current state of atmospheric sea-salt budget estimation, especially the long range transport rate of sea-salt aerosols from world oceans to ice or land surfaces, running this aerosol model with a three-dimensional climate model is necessary to provide a more accurate account of the sea-salt aerosol cycle in the atmosphere.

Acknowledgments. Funding for the University of Miami aerosol measurements was provided by Heimaey, Iceland—NOAA cooperative agreement NA90RAH00075; Oahu, Hawaii—NASA contracts NAG8-621, NAG8-841, and NAG1-1229; National Science Foundation as part of the Sea-Air Exchange program; Mace Head and Bermuda—National Science Foundation grants ATM-8703411, ATM-9013125, ATM9414846; and Palmer Station—U.S. Department of Energy contracts DEAC1791EV90116 and DEAC1794EV901. The authors acknowledge support from the Cape Grim Baseline Air Pollution program managed jointly by the Australian Bureau of Meteorology and CSIRO, the CGBAPS staff for many years of untiring logistical support, and the Australian Government Analytical Laboratories (Kingston) for the aerosol analysis. Finally, the authors would like to express their sincere thanks to G. Issac and R. Leaitch for their valuable comments during an internal review at Atmospheric Environment Service, Environment Canada.

References

Barrie, L. A., Arctic aerosols: Composition sources and transport, in *Advanced Studies Workshop on Ice Core Studies of Global Biogeochemical Cycles*, edited by R. Delmas, *NATO ASI Ser. I Global Environ. Change*, *30*, 1–23, 1995.

Barrie, L. A., and M. J. Barrie, Chemical compositions of lower tropospheric aerosols in the high Arctic, *J. Atmos. Chem.*, *11*, 211–226, 1990.

Barrie, L. A., R. Staebler, D. Toom, B. Grorgi, G. den Hartog, S. Landsberger, and D. Wu, Arctic aerosol size-segregated chemical observations in relation to ozone depletion during Polar Sunrise Experiment 1992, *J. Geophys. Res.*, *99*(D12), 25,439–25,451, 1994.

Baumgartner, A., and E. Reichel, *The World of Water Balance*, Elsevier Sci., New York, 1975.

Blanchard, D. C., The electrification of the atmosphere by particles from bubbles in the sea, in *Progress in Oceanography*, vol. 1, edited by M. Sears, pp. 71–202, Pergamon, New York, 1963.

Eriksson, E., The yearly circulation of chloride and sulfur in nature: Meteorological, geochemical and padological implications, 1, *Tellus*, *11*(4), 375–403, 1959.

Eriksson, E., The yearly circulation of chloride and sulfur in nature: Meteorological, geochemical and padological implications, II, *Tellus*, *12*(1), 63–109, 1960.

Erickson, D. J., and R. A. Duce, On global flux of atmospheric sea salt, *J. Geophys. Res.*, *93*(C11), 14,079–14,088, 1988.

Erickson, D. J., J. T. Merrill, and R. A. Duce, Seasonal estimates of global atmospheric sea-salt distributions, *J. Geophys. Res.*, *91*(D1), 1067–1072, 1986.

Fergusson, J. E., *Inorganic Chemistry and the Earth*, Pergamon, New York, 1982.

Gong, S. L., L. A. Barrie, and J.-P. Blanchet, Modeling sea-salt aerosols in the atmosphere, 1, Model development, *J. Geophys. Res.*, this issue.

Jaenicke, R., Tropospheric aerosols, in *Aerosol-Cloud-Climate Interactions*, edited by P. Hobbs, pp. 1–31, Academic, San Diego, Calif., 1993.

Jobson, B. T., H. Niki, Y. Yokouchi, J. Bottenheim, F. Hopper, and R. Leaitch, Measurements of C_2-C_6 hydrocarbons during the Polar Sunrise 1992 Experiment: Evidence for Cl atom and Br atom chemistry, *J. Geophys. Res.*, *99*(D12), 25,355–25,368, 1994.

McFarlane, N. A., G. J. Boer, J.-P. Blanchet, and M. Lazare, The Canadian climate centre second-generation general circulation model ant its equilibrium climate, *J. Clim.*, *5*, 1013–1044, 1992.

Monahan, E. C., D. E. Spiel, and K. L. Davidson, A model of marine aerosol generation via whitecaps and wave disruption, in *Oceanic Whitecaps*, edited by E. C. Monahan and G. Mac Niocaill, pp. 167–174, D. Reidel, Norwell, Mass., 1986.

Mozurkewich, M., Mechanisms for the release of halogens from sea salt particles by free radical reactions, *J. Geophys. Res.*, *100*(D7), 14,199–14,207, 1995.

Petrenchuk, O. P., On the budget of sea salts and sulfur in the atmosphere, *J. Geophys. Res.*, *85*(C12), 7439–7444, 1980.

Slinn, S. A., and W. G. N. Slinn, Modeling of atmospheric particulate deposition to natural waters, in *Atmospheric Pollutants in Natural Waters*, edited by S. J. Eisenreich, pp. 23–53, Ann Arbor Sci., Ann Arbor, Mich., 1981.

Spillane, M. C., E. C. Monahan, P. A. Bowyer, D. M. Doyle, and P. J. Stabeno, Whitecaps and global fluxes, in *Oceanic Whitecaps*, edited by E. C. Monahan and G. Mac Niocaill, pp. 209–218, D. Reidel, Norwell, Mass., 1986.

Therrien, D., Le modèle de circulation générale atmosphérique Canadien en version colomne: FIZ-C, M.S. thesis, 123 pp., Univ. of Quebec at Montreal, 1993.

Van Loon, H., *Climates of the Oceans*, *World Surv. Climatol.*, vol. 15, Elsevier, New York, 1984.

G. P. Ayers, Division of Atmospheric Research, Private Bag No. 1, Mordialloc, Victoria 3195, Australia.

L. A. Barrie and S. L. Gong, Atmospheric Environment Service, 4905 Dufferin Street, Downsview, Ontario, Canada M3H 5T4. (e-mail: lbarrie@dowsu01.dow.on.doe.ca)

J.-P. Blanchet and L. Spacek, Earth Sciences Department, University of Quebec at Montreal, P.O. Box 8888, Station "Centre Ville," 515 Ste-Catherine St., Montreal, Quebec, Canada H3C 3P8.

J. M. Prospero and D. L. Savoie, Rosenstiel School of Marine and Atmospheric Sciences, University of Miami, 4600 Rickenbacker Causeway, Miami, FL 33149-1098.

(Received February 3, 1996; revised October 11, 1996; accepted October 11, 1996.)